^{23}Na Spin-Lattice Relaxation Measurements in Dehydrated Na-X Zeolite*

Mutsuo Igarashi[a], Noriaki Okubo[b], Shuichi Hashimoto[c], Ryozo Yoshizaki[d], and Deok Joon Cha**[e]

[a]Department of Applied Physics, Gunma College of Technology, Gunma 371, Japan
[b] Institute of Physics, University of Tsukuba, Ibaraki 305, Japan
[c] Chemistry Department, Gunma College of Technology, Gunma 371, Japan
[d] Institute of Applied Physics, University of Tsukuba, Ibaraki 305, Japan
[e] Department of Physics, Kunsan National University, Kunsan 573-360, R. O. Korea

Z. Naturforsch. **51 a,** 657–661(1996); received October 17, 1995

The spin-lattice relaxation time T_1 of ^{23}Na-NMR in a dehydrated Na-X zeolite has been measured from 20 to 300 K. The recovery curve is not single-exponential at all measured temperatures and T_1^{-1} increases with the square of temperature around room temperature. The results are analyzed by assuming non-equivalent sites and by applying the theory of the Raman process based on covalency.

Key words: Dehydrated Na-X zeolite; ^{23}Na-NMR; spin-lattice relaxation; Raman process; nonequivalent sites.

1. Introduction

Zeolites can adsorb many kinds of atoms and molecules in the open space called micro cage. They sometime show ferromagnetism [1], semiconductivity [2], and so on. Zeolites consist of a number of AlO_4^-- and SiO_4-tetrahedra linked by O atoms and cations such as Na^+ included to compensate the residual negative charge. The cations play an important role for the adsorption [3]. The capability of adsorption depends on the concentration of cation which is controlled by the ratio of the numbers of Al and Si atoms.

In one of zeolites called faujasite Na-X (Na_{86}-$[(AlO_2)_{86}\cdot(SiO_2)_{106}]\cdot 264H_2O$ [4]), the location of the Na atoms and the interaction with their environment have been examined with several techniques; X-ray diffraction [5], neutron diffraction [6], far infrared [7], NMR [8, 9] and so on. The location of the Na atoms is expected to have a large effect on the spin-lattice relaxation in ^{23}Na-NMR. However, to the authors knowledge, such a dynamical study has not yet ever been done.

In this paper we report a study of the spin-lattice relaxation of the ^{23}Na-NMR in dehydrated Na-X zeolite.

2. Experimental

The powder sample of Na-X (F-9 #100, product of Toso Inc. as catalyst) was used without further purification. About 2 g of it were heated at 573 K in vacuum for 8 hours to dehydrate and then the material was sealed in a glass ampule of 10 mm diameter without exposure to air.

^{23}Na-NMR measurement was done at 7 T (Oxford superconducting magnet). The signal was observed with a spectrometer (Matec 5100 pulse power amplifier and 525 receiver). The signal was recorded with a signal averager and transferred to a computer through a GP-IB line for processing. The temperature was controlled within 0.1 K, but the accuracy was 1 K.

The central transition of the ^{23}Na-NMR, fairly broadened by quadrupolar interaction was observed. Since the FID signal could hardly be observed, the spin echo signal was employed to measure the spin-lattice relaxation. The pulse sequence used was $\pi/2$ - variable delay - $\pi/2$ - τ - π.

---

* Presented at the XIIIth International Symposium on Nuclear Quadrupole Interactions, Providence, Rhode Island, USA, July 23-28, 1995.

** Research supported by the KNU Fund in 1995.

Reprint requests to Dr. M. Igarashi.

0932-0784 / 96 / 0500-0657 $ 06.00 © – Verlag der Zeitschrift für Naturforschung, D-72072 Tübingen

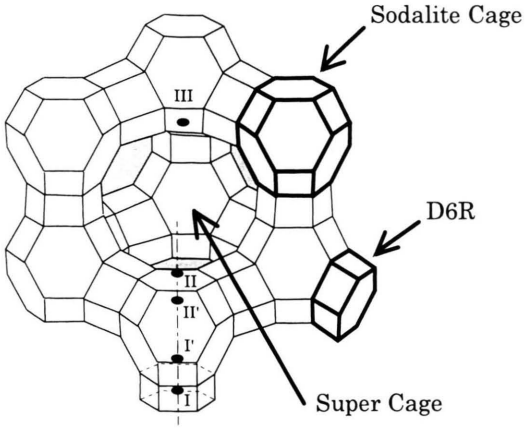

Fig. 1. The crystal structure of Na-X Zeolite. Fourteen-faced polyhedra of SiO_2 (Sodalite Cage) are connected by doubled six-membered rings (D6R). The sites of cation[10] are shown by small circles.

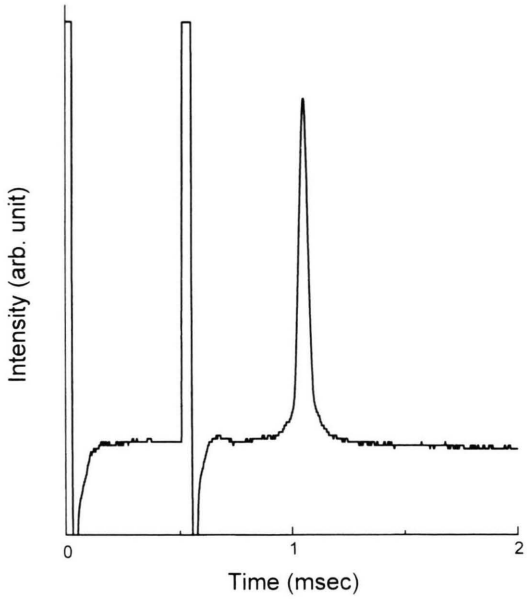

Fig. 2. An example of the spin echo signal. At 80K, repeat time 10 sec, 256 times averaging.

3. Results and Discussion

3.1. Echo Shape

The crystal structure of Na-X (space group Fd3m [4]) is schematically shown in Figure 1. A fourteen-faced basic unit (sodalite cage or β cage) is connected with four neighbouring basic units through doubled six membered rings (D6R). Among the basic units there is one large space called super cage. For Na atoms there are five sites as shown in Figure 1. The quadrupole coupling constants of their nuclei have been determined using the double-rotation NMR (DOR) technique [10]. The asymmetry parameter η can not be determined by the technique. The quadrupole coupling constants P_Q defined by

$$P_Q = \frac{e^2qQ}{h}\sqrt{1+\frac{\eta^2}{3}} \qquad (1)$$

are shown in Table 1. Since site I is located at the center of the D6R and the symmetry of the environment is highest, this site has the smallest quadrupole coupling constant. Sites I' and II' are inside the sodalite cage and correspond to the middle range values. Since sites II and III face the super cage and have the lowest symmetry, these sites correspond to the largest coupling constants. In our spin-echo experiments, the observed NMR signal is a sum of the contribution from these sites. For simplicity, we separate Na sites into three groups with respect to the magnitude of the quadrupole coupling constant.

Site	P_Q (MHz)
I	0.4
I'	2.3
II	4.2
II'	2.3
III	4.7

Tab. I. Quadrupole coupling constants $P_Q = (e^2qQ/h)(1+\eta^2/3)^{1/2}$ of the five nonequivalent sites of sodium atoms (Ref. 10).

Small coupling group: site I (P_Q = 0.4MHz),
Middle coupling group: site I', II' (P_Q = 2.3MHz),
Large coupling group: site II, III ($P_Q \simeq$ 4.5MHz).

An example of the spin echo signal is shown in Figure 2. The width of the line due to the central transition is approximately proportional to the square of the quadrupole coupling constant [11]. Since the width of the echo is inversely proportional to the line width, the sharp echo signal corresponds to the middle and large coupling groups. On the other hand, the fairly broad signal noticed on the bottom of the figure is considered to correspond to the small coupling group. Since the transition probability for the quadrupole relaxation is proportional to the square of the coupling constant, the broad echo may have fairly large time constant. However, the magnetization recovery curve hardly changed even by lengthening of the waiting time. It is very difficult to measure such

a long T_1 for site I because it requires a high stability of the apparatus together with a good signal-to-noise ratio over a long time. Thus the attention was focused only on the sharp echo signal, and the relaxation time was measured with a sufficiently long waiting time for the sharp echo. For simplicity the base line was chosen as that far from the echo.

3.2. Magnetization Recovery

Since the quadrupole coupling of ^{23}Na nuclei with the environments is fairly large, the quadrupolar relaxation is expected to be dominant. For the system of spin $I = 3/2$, the magnetization recovery for one site is then expressed by the following equation [12]:

$$R_c(t) = \frac{M_c(\infty) - M_c(t)}{M_c(\infty)} = \frac{1}{2}\exp(-2W_1 t) + \frac{1}{2}\exp(-2W_2 t), \quad (2)$$

where $M_c(t)$ is the nuclear magnetization corresponding to the central transition at time t after saturation and W_1 and W_2 are the transition probabilities corresponding to $\Delta m = \pm 1$ and $\Delta m = \pm 2$, respectively[13]. Thus the recovery curve is generally not single-exponential. Since W_1 and W_2 depend on the orientation of the crystal to the external magnetic field, for the powder sample they must be averaged with respect to orientation.

Unless there is an other prominent mechanism, the relaxation is dominated by the Raman process [14]. That this is the case for the present substance is shown later by the temperature dependence of the relaxation time. Kranendonk calculated the relaxation rate in alkali halides, using a point charge model and pointed out the importance of covalency [15]. Yosida and Moriya calculated it on the base of covalency but their values did not reach the experimental ones [16]. However it was recently shown that the relaxation of NQR in several kinds of metal halides can be explained by Yosida and Moriya's theory [17, 18, 19]. When this theory is applied to the present case, one can show that W_1 and W_2 become equal to each other after the orientation average [20]. Then, if there is one site, the recovery curve should be single-exponential, whereas the observed recovery curves were multi-exponential. A typical magnetization recovery is shown in Figure 3. Therefore this is attributed to the existence of several sites.

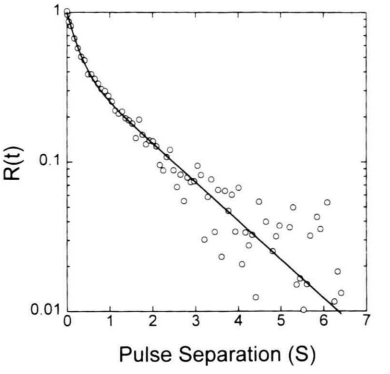

Fig. 3. A typical magnetization recovery of the central transition at 80 K. The curve shows the fitting of (2).

Since, in Na-X, the concentration of Al is lower than that of Si, there are many sites wihch are not occupied by Na atoms. In fact a typical value of T_2 was 3.1 ± 0.4 msec and this is rather large, so that the dipolar interaction among the ^{23}Na nuclei is considered to be small. Then the magnetization of each site recovers independently.

One can obtain the ratios of the number of Na sites by counting them in one cage because all sodalite cages are equal. Since the numbers of site I, I', II, II', and III in one cage are 2, 4, 4, 4, and 6, respectively, the ratio of the sites of large and middle coupling groups is given by (Site II and III) : (Site I' and II'), that is, 5 : 4. If all the sites are occupied by Na atoms with equal weight, the contribution of the magnetization from each site is proportional to the number of the sites.

Then the magnetization recovery curve is represented with short and long relaxation times T_{1s} and T_{1l} as follows:

$$R(t) = a\exp\left(-\frac{t}{T_{1s}}\right) + (1-a)\exp\left(-\frac{t}{T_{1l}}\right), \quad (3)$$

where a represents the relative weight of the large coupling group which is equal to 5/9. The fitting of (3) to the experimental recovery curve was performed with fixing a as 0.56 to obtain the solid curve in Figure 3. Such an excellent fit was obtained at all measured temperatures. This supports the present treatment.

3.3. Temperature Dependence

Two relaxation times T_{1s} and T_{1l} obtained as the fitting parameters are shown in Figure 4. The solid lines are eyeguides which are drawn to pass the data

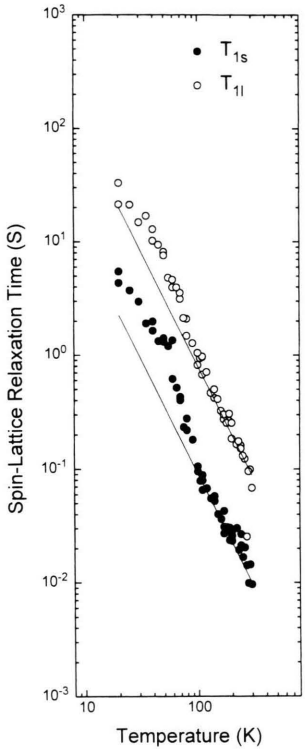

Fig. 4. Temperature dependence of two relaxation times T_{1s} and T_{1l}.

points at room temperatures with a slope of 2. Both T_1's show T^2 dependence above 100 K and stronger dependence with decreasing the temperature. This behaviour is typical for relaxation due to the Raman process. However, below 50 K the dependence becomes weak. In case of alkali halide crystals, even magnetic impurities of ppm order make T_1 shorter than otherwise [14]. Since the purity of the sample used in the present study was not high, the weakening of the temperature dependence of the T_1's below 50 K may also be attributed to impurities.

The rate of the relaxation due to the Raman process is expressed by [20]:

$$(T_1T^2)^{-1} = (\tau\theta_D^2)^{-1} \sum_{\nu} \varepsilon_\nu D_\nu(T^*), \tag{4}$$

where

$$\tau^{-1} = \frac{3e^4Q^2 < r^{-3} >^2 c^3}{100\pi^3 a^7 d^2 v_s^3} T^{*2} N_{11}, \tag{5}$$

$$D_\nu(T^*) = T^* \int_0^{1/T^*} \frac{x^2 e^x}{(e^x - 1)^2} L_\nu(cT^*x)\,\mathrm{d}x, \tag{6}$$

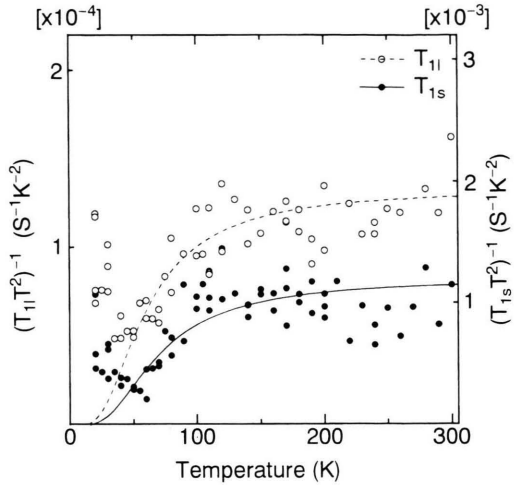

Fig. 5. Temperature dependence of $(T_{1s}T^2)^{-1}$ and $(T_{1l}T^2)^{-1}$. The curves show the fittings of (3).

where a denotes the distance of the Na atom in question from the bonding atoms, d the density of the crystal, v_s the sound velocity. $\langle r^{-3} \rangle$ means the expectation value of r^{-3} with respect to the p electron of the Na atom. c is defined as $c = k_D a$ with the maximum wave number k_D. N_{11} depends on covalency and increases with increase of the number of the bonds [20]. T^* is the temperature divided by the Debye temperature θ_D. $D_\nu(T^*)$ involves a structure dependent function $L_\nu(cT^*x)$ and has a temperature dependence similar to that of Debye's specific heat[21]. $D_\nu(T^*)$ is summed up about the bond pairs with the weight ε_ν. The value $(T_1T^2)^{-1}$ is nearly constant above θ_D and decreases to zero with decreasing of temperature.

$(T_{1s}T^2)^{-1}$ and $(T_{1l}T^2)^{-1}$ are plotted against the temperature in Figure 5. The fitting of (4) was done to the data except below 50 K, using the effective bond pairs.

3.4. Concluding Remarks

We now consider the ratio T_{1s} and T_{1l}. Since the quadrupolar relaxation is proportional to the square of the quadrupole coupling constants, for the ratio T_{1s}^{-1}/T_{1l}^{-1} we expect a value of $(4.5/2.3)^2 \simeq 4$, whereas the obtained value is typically 8. However when the relaxation is attributed to the Raman process, other factors must be taken into account. The most effective bonds to the relaxation of ^{23}Na nuclei are those with O atoms from the consideration

of their electronegativities. The number of the nearest O atoms is 4 at site III, while 6 at other sites. Moreover a differs from site to site [6]. These bring about difference in N_{11} at each site. Therefore, to compare the absolute magnitude of the T_1's, further consideration about these factors is required. As a conclusion, most features of the relaxation of ^{23}Na-NMR in Na-X zeolite could be explained with the theory of the Raman process based on covalency by assuming non-equvalent sites.

[1] Y. Nozue, T. Kodaira, O. Terasaki, K. Yamazaki, T. Goto, D. Watanabe, and J. M. Thomas, J. Phys. Condens. Matter **2,** 5209 (1990).
[2] N. Herron, Y. Wang, M. M. Eddy, G. Stucky, D. E. Cox, K. Moller, and T. Bein, J. Amer. Chem. Soc. **111,** 530 (1989).
[3] O. Terasaki, Solid State Phys. (in Japanese) **27,** 601 (1992).
[4] D. W. Breck, Zeolite – Molecular Sieves –, Wiley, New York 1973, pp. 176.
[5] W. J. Mortier, E. Van den Bossche, and J. B. Uytterhoeven, Zeolites **4,** 41 (1984).
[6] A. N. Fitch, H. Jobic, and A. Renouprez, J. Phys. Chem. **90,** 1311 (1986).
[7] M. D. Baker, J. Godber, and G. A. Ozin, J. Amer. Chem. Soc. **107,** 3033 (1985).
[8] G. A. H. Tijink, R. Janssen, and W. S. Veeman, J. Amer. Chem. Soc. **109,** 7301 (1987).
[9] R. Challoner and R. K. Harris, Zeoltes **11,** 265 (1991).
[10] H. A. M. Verhulst, W. J. J. Welters, G. Vorbeck, L. J. M. van de Ven, V. H. J. de Beer, R. A. van Santen, and J. W. de Haan, J. Phys. Chem. **98,** 7056 (1994).
[11] J. F. Baugher, P. C. Taylor, T. Oja, and P. J. Bray, J. Chem. Phys. **50,** 11 (1069).
[12] G. Bonera, F. Borsa, and A. Rigamonti Phys. Rev. B **2,** 2784 (1970).
[13] E. R. Andrew and D. P. Tunstall, Proc. Phys. Soc. London **78,** 1 (1961).
[14] R. V. Pound, Phys. Rev. **79,** 685 (1950).
[15] J. Van Kranendonk, Physica **20,** 781 (1954).
[16] K. Yosida and T. Moriya, J. Phys. Soc. Japan **11,** 33 (1956).
[17] N. Okubo, H. Sekiya, C. Ishikawa, and Y. Abe, Z. Naturforsch. **47a,** 713 (1992).
[18] N. Okubo and Y. Abe, Z. Naturforsch. **49a,** 680 (1994).
[19] N. Okubo, M. Igarashi, and R. Yoshizaki, Z. Naturforsch. **50a,** 737 (1995).
[20] N. Okubo, M. Igarashi, R. Yoshizaki, Z. Naturforsch. **51a,** 267 (1996).
[21] C. Kittel, Introduction to Solid State Physics, John Wiley Inc., New York 1976.